Inherent safety aspects of metal fuelled FBR

T. Sathiyasheela*, A. Riyas, R. Sukanya, P. Mohanakrishnan, S.C. Chetal

Indira Gandhi Centre for Atomic Research, Kalpakkam 603 102, Kanchipuram District, Tamil Nadu, India

HIGHLIGHTS

Inherent safety of metal fuelled FBR is studied by static and dynamic methodology of reactor physics and thermal-hydraulics. ► It is discovered that FBR with metal fuel is inherently safe against ULOFA.

► Sensitive parameters are core radial expansion feedback, sodium void effect and flow halving time.

► Sensitivity analyses are carried out with 20% uncertainty.

► Inherent safety of 1000 MWe with the extended flow coast down is recommended to avoid cliff edge effects.

ARTICLE INFO

ABSTRACT

Static and dynamic studies of metal fuelled fast breeder reactors (MFBR) are carried out to verify the passive shutdown capability and its inherent safety parameters. Static calculations are carried out to determine the vested reactivity feedback parameters from the fuel and coolant temperature rise separately. Power reactivity decrement of metal fuel reactor is found to be small as compared to oxide fuel reactor of same size.

ULOF analysis of metal (U–Pu–6% Zr) 1000 MWe pool type MFBR is studied with a flow halving time of 8 s. The study is also made with considering uncertainties on the sensitive feedback parameters such as core radial expansion feedback and sodium void reactivity effect. Inference of the study is, nominal transient behaviour of 1000 MWe core is benign under unprotected loss of flow accident (ULOFA) and the transient power reduces to natural circulation based Safety Grade Decay Heat Removal System (SGDHRS) capacity before the initiation of boiling. From the study, it is concluded that if the sodium void reactivity is limited (4.6$) then the inherent safety of 1000 MWe design is assured, even with 20% uncertainty on the sensitive parameters and also it is found out higher primary pump flow halving time (15 s instead of 8 s) can avoid cliff edge effects in 1000 MWe MFBR transient behaviour.

1. Introduction

Metal fuel was the original choice of fast breeder reactor as it is compatible with liquid sodium in the earlier sixties (Wigeland and Cahalan, 2009). But, it was perceived that it was very difficult to achieve high burn up due to irradiation induced swelling. However, EBR-II continued its operation with Mark-1 metal fuel. Based on the experience gained in Mark-I fuel of EBR-II, there are many modifications carried out to achieve high burn up (Chang, 2007). Later on plutonium was included in the fuel matrix to introduce the breeding concept. With all the modifications higher burn up and higher breeding was made to be possible with metal fuel. With respect to safety, liquid metal fast breeder reactor (LMFBR) systems employ defends in depth approach to protect the reactor, multiple barriers to prevent the release of radiation, highly reliable system for controlling and protecting the plant, high quality construction and rigorous maintenance exhaustive training certification of the operators (Wade et al., 1997). Engineered safety systems are available to protect the reactor from the design basis events. These kind of active safety systems are highly reliable, but in case the switching systems fails or any multiple component failure may leads to untoward result. So, it is necessary to have passive safety systems which will bring the reactor to safe shut down and removes the decay heat by invoking nuclear, thermo-hydraulic and mechanical feedbacks. Inherent safety of the system provides passive safety control. Inherent safety is the capability of the reactor system to preclude hypothetical core disruptive accidents without requiring shutdown using engineered safety system or operator intervention to keep the reactor in safe conditions. Inherent safety capability of the reactor is likely helpful in removing costly engineered safety

* Corresponding author at: Reactor Neutronics Division, Reactor Engineering Group, IGCAR, Kalpakkam 603 102, India. Tel.: +91 44 27480088; fax: +91 44 27480096.

E-mail addresses: thangavel.sathiyasheela@gmail.com, sheela@igcar.gov.in (T. Sathiyasheela), rias@igcar.gov.in (A. Riyas), kanya@igcar.gov.in (R. Sukanya), Mohan_parat@yahoo.com (P. Mohanakrishnan), dir@igcar.gov.in (S.C. Chetal).

Nomenclature

A	power-flow coefficient
A_f	flow area (cm^2)
B	power/flow coefficient
C	inlet temperature coefficient
Cc	specific heat capacity of coolant ($J/g/°C$)
C^i	reactivity due to core boundary movement axially per unit length of core (pcm/cm)
D^j	reactivity coefficient per unit boundary movement of the core in to radial blanket at a given axial location (pcm/cm)
$E^j_{1,2}$	reactivity coefficient per unit boundary movement of the first enrichment zone to second at a given axial location (pcm/cm)
$E^j_{2,3}$	reactivity coefficient per unit boundary movement of the first enrichment zone to second at a given axial location (pcm/cm)
F	normalised flow
$irc1$	channel separating core-1 and core-2
$irc2$	channel separating core-2 and core-3
P	normalised linear power
$q^{j,i}$	linear power corresponds to the nominal power at a given location
R_1	Radius of the first enrichment zone (cm)
R_2	Radius of the second enrichment zone (cm)
R_c	Radius of the core (cm)
h_{fs}	effective heat transfer between fuel and clad ($W/cm/°C$)
h_{sc}	effective heat transfer between clad and coolant ($W/cm/°C$)
v	flow velocity (cm/s)
W^j	weighting factor calculated based on cantilever bending model
ρ	density of coolant (g/cm^3)
$\delta\rho_D$	Doppler effect feedback $(\delta\rho_D/\delta t) = (K_D/T)$; where K_D is Doppler constant (pcm)
$\delta\rho_{fax-expn}$	fuel axial expansion reactivity feedback (pcm)
$\delta\rho_{cax-expn}$	clad axial expansion reactivity feedback (pcm)
$\delta\rho_{Na}$	bulk coolant expansion reactivity feedback (pcm)
$\delta\rho_{frad-expn}$	fuel radial expansion reactivity feedback (pcm)
$\delta\rho_{crad-expn}$	clad radial expansion reactivity feedback (pcm)
$\delta\rho_{fax-bound}$	fuel axial boundary movement reactivity feedback (pcm)
$\delta\rho_{fax} = \delta\rho_{fax-expn} + \delta\rho_{fax-bound}$	net fuel axial reactivity feedback (pcm)
$\delta\rho_{core1-core2}$	fuel radial boundary (from core-1 to core-2) movement reactivity feedback (pcm)
$\delta\rho_{core2-core3}$	fuel radial boundary (from core-2 to core-3) movement reactivity feedback (pcm)
$\delta\rho_{core3-blkt}$	fuel radial boundary (from core-3 to blkt) movement reactivity feedback (pcm)
$\delta\rho_{rd}$	control rod drive line expansion (pcm)
$\delta\rho_g$	grid plate expansion (pcm)
$\delta\rho_v$	vessel expansion (pcm)
α_f	fuel thermal expansion coefficient ($°C^{-1}$)
α_s	clad thermal expansion coefficient ($°C^{-1}$)
α_{Na}	coolant thermal expansion coefficient ($°C^{-1}$)
α_{rd}	control rod drive line expansion coefficient
Δk_f	fuel reactivity worth per mesh (pcm)
Δk_s	clad reactivity worth per mesh (pcm)
Δk_{Na}	coolant reactivity worth per mesh (pcm)
ΔT_{Na}	difference in coolant temperature between the given axial node and inlet coolant temperature ($°C$)
δq	change in linear power between two asymptotic states (W/cm)
δT_f	change in fuel temperature between two asymptotic states ($°C$)
δT_s	change in clad temperature between two asymptotic states ($°C$)
δT_{Na}	change in coolant temperature between two asymptotic states ($°C$)
δT_{jsp}	change in coolant temperature between two asymptotic states at the spacer pad location ($°C$)
δT_{out}	change in outlet coolant temperature ($°C$) due to change in P/F ratio
$\Delta\rho_{ext}$	external reactivity

system or it can act as a stand by system to provide confidence to the reactor designer.

Inherent safety of fast reactors pertains to the transient behaviour of the reactor in two respects (Ott, 1988). One is the short term response to a major perturbation in coolant capability or power production. Second one is the long term response, reaching a safe asymptotic state with time. The goal of the short term response is to keep the elevated temperature below the damaging limit, and in the long term, asymptotic states temperatures below the stress induced creep failure, etc. Analysis of Anticipated Transient Without Scram (ATWS) such as loss of coolant flow, loss of heat sink and transient over power are available in the literature (Cahalan et al., 1990; Royl et al., 1990; Yokoo and Ohta, 2002) for both metal and oxide fuel. From the results it is confirmed that due to lower excess reactivity and control rod worth, Unprotected Transient Over Power (UTOP) incidents are less severe in metal cores as compared to oxide cores and also larger temperature margin is available to coolant boiling. From the response to a small reactivity perturbations of a medium sized reactors studied using frequency and time domain analysis (Singh et al., 1993) it is learnt, metal fuel core is more sensitive to a small reactivity perturbations than oxide, but both the core satisfy the linear stability criteria.

Based on the available results in the literature and comparisons of metal and oxide fuel, metal fuel is found to be inherently safe for the major unprotected accidents. Neutronic and thermo physical properties of both the fuel are compared in our earlier paper (Sathiyasheela et al., 2011). The main differences relevant to the inherent safety are the better thermo-physical properties such as high density and high thermal conductivity. Compatibility of metal fuel with liquid sodium increases the gap conductance. Thus the thermal time constant (Hummel and Okrent, 1970), i.e., the time taken for the temperature difference across the fuel pin to decrease by a factor of $1/e$ is very small and that makes the temperature swing between zero power and nominal power is relatively small. So the temperature dependent Doppler reactivity does not swing much between the zero power and nominal power. Consequently the reactivity loss during start up is reduced and the positive reactivity insertion during power decay is also reduced. This contributes to the small power reactivity decrement, i.e., the amount of reactivity required to bring the reactor to zero power during Unprotected Loss of Flow Analysis (ULOFA).

To asses the consequence of the unprotected transients due to a major perturbation, it is necessary to carry out a detailed dynamic analysis by considering all feedbacks. From the static analysis carried out by Singh et al. (1994), it is learnt both metal and carbide fuel with sodium bond gap provide passive safety as compared to oxide fuel with helium bond gap material. It is also found out, though the sodium void coefficient of metal fuel is high, the pre-disassembly lost longer (Singh and Harish, 2002) in metal fuels as compared to

carbide and oxide fuels. But, before getting into the detailed safety analysis it is better to find the safety parameters and the maximum possible temperature for series of typical probable events. Outcome of static analysis such as the power coefficient and temperature coefficient will provide a base to understand consequence of such probable events. Power coefficient is nothing but a change in reactivity for a unit change in power. Power coefficient calculations using lumped parameter are carried out and explained in our earlier paper (Sathiyasheela and Mohanakrishnan, 2011). But it does not give any idea about, how much is the reactivity vested from the coolant side and how much is comes from the fuel side. It is understood from the literature that (Wade and Fujita, 1989; Ott, 1988; Wade and Chang, 1988; Planchon, 1987), if the vested reactivity from the coolant side is more, this will allow more neutron to leak out and take the reactor to an asymptotic state during ULOFA. So, in the present study, methodology is developed to find out the vested reactivity from the fuel side and coolant side separately and also to find out the power reactivity decrement when the power is taken from nominal power to zero power. From the reactivity parameter inherent safety capability of the reactor and the maximum possible coolant temperature is also derived.

Reactivity feedback parameters were calculated earlier (Wade and Fujita, 1989; Ott, 1988; Wade and Chang, 1988) without considering the boundary movement of the reactor. In the present work, other than the thermal radial expansion, radial boundary movement of core-1 material into to core-2, core-2 material into to core-3 and core-3 material in to radial blanket due to thermal expansion is also considered (Harish et al., 1999). The corresponding reactivity loss/gain is also taken in to account in the power reactivity decrement calculation. Similarly, axial boundary movement of lower axial blankets into core, and the core into upper axial blankets are also considered. Reactivity feedback parameters of medium sized 500 MWe oxide fuel core (PFBR) and metal fuel core are calculated and compared. It is found reactivity decrement of metal fuel reactor is small as compared to oxide fuel. So, metal fuel can goes to sub-critical state with comparatively smaller negative feedback reactivity during ULOFA, and its maximum coolant temperature is below its saturation.

ULOFA analyses of 500 MWe metal core reactor was carried out (Harish et al., 2009) and concluded that sodium boiling is delayed even after considering uncertainties in feedback reactivity effects. If the Safety Grade Decay Heat Removal System (SGDHRS) is able to remove decay heat after 20 min, further increase in sodium voiding or coolant temperature increase can be prevented. It is possible to design natural circulation based SGDHRS with capacity >2.5% of thermal power (Chetal et al., 2006). Thus the SGDHRS capacity of 1000 MWe case is taken as 67 MWt in the present study at the nominal temperature of hot pool at full power. It may be noted that SGDHRS capacity during transient increases when reactor outlet and hot pool temperatures rise.

U–Pu–Zr alloys prevent the U–Pu interaction with clad. Addition of Zr increases fuel melting point and slightly reduces conductivity. While both 10% Zr and 6% Zr content have been tested in the past, metal fuel with 6% Zr is chosen here, because of its higher breeding capacity. In the present work, ULOF analyses are carried out for MFBR (U–Pu–6% Zr) 1000 MWe (2632 MWt) reactors to verify the passive shutdown capability of the reactor. The present study is also check the passive shutdown capability of the reactor with the inclusion of uncertainties on sensitive feedback parameters such as core radial expansion reactivity feedbacks and sodium void reactivity effect. Typical uncertainty in reactivity coefficients are about 20% (Mueller, 1986; Lehto et al., 1987). The cross-section set (Devan, 2003; Manturov, 1997) and the computer codes of IGCAR were used recently in BN-600 benchmark core analysis where experimental data on sodium void reactivity effect in BFS62-3A experimental set up was also compared with predictions (IAEA-TECDOC-1623,

Table 1
Parameters of 1000 MWe core.

Efficiency	(%)	38
Assembly pitch	(cm)	16.8
Blanket pin diameter	(cm)	1.275
Clad material	(SS)	Modified 9Cr–1Mo (Grade 91)
Clad thickness – blanket	(cm)	0.06
Clad thickness – fuel	(cm)	0.053
Fuel pin diameter	(cm)	0.8
Fuel pins per sub-assembly		271
Maximum linear heat rating	(W/cm)	500
Number of CSR/DSR		18/6
Number of rows of radial blanket		2
Number of sub-assemblies in core-1/core-2/core-3		79/96/72
Number of sub-assemblies in radial blanket		198
Pins per blanket sub-assembly		127
Pu enrichment core-1/core-2/core-3	(%)	11.05/12.25/16.60
Total axial blanket height	(cm)	30 + 30 = 60
Volume fractions of fuel/steel/sodium – core region	(%)	41.94/23.16/34.9
Volume fractions of fuel/steel/sodium – radial blanket	(%)	54.44/19.88/25.68
Coolant void worth	(pcm)	2357 (5.6$)
Doppler worth	(pcm)	−538
Core inlet/outlet temperature	(°C)	365/554
Total coolant flow rate	(kg/s)	13,670
Type of primary system		Pool type

2010). An uncertainty of 16% was found. Still, we have assumed 20% uncertainty in sodium void reactivity effect along with 20% uncertainty of radial expansion reactivity feedback. Presently analysis has been done with data for fresh core. With core burn up, reactivity feedback coefficients can change. For example, sodium void reactivity effect tends to increase. It is expected that, due to swelling of hex-can with irradiation, free expansion of core with temperature gets restricted, resulting in possible reduction of radial expansion reactivity feedback. Thus we have considered a case of higher uncertainty of 50% in radial expansion reactivity feedback also.

Another important design parameter to achieve inherent safety is the extended flow coast down (Coffield et al., 1986). ULOF analyses are carried out with a higher flow halving time of 15 s. With higher flow halving time, even with 20% uncertainties on sensitive feedback parameters such as core radial expansion feedback and sodium void reactivity the reactor goes to sub-critical and the transient power reduces to SGDHR system capacity. From the study it is concluded that, for ensuring the safety of 1000 MWe MFBR core, with considering the uncertainties, either a reduction of Na void reactivity effect or increase in flow halving time is required. Higher primary pump flow halving time (15 s instead of 8 s) can avoid cliff edge effects in 1000 MWe MFBR transient behaviour.

2. Reactor description

1000 MWe (2632 MWt) core is divided in to three enrichment zones, with properly chosen enrichment to achieve power flattening. 247 fuel subassemblies are distributed in these three cores viz., core-1 with 79 subassemblies, core-2 with 96 subassemblies core-3 with 72 subassemblies respectively. There are 271 pin per subassembly in the core and 127 pin per subassembly in the blanket. Fuel sub-assembly pitch is 16.8; the flow area is about 76 cm^2. Core inlet and outlet temperatures are 365/554 °C. Flow rate in the central sub-assembly is about 49 kg/s. Out of the total flow through reactor of 13,670 kg/s, 12,440 kg/s pass through the sub assemblies. The relevant core parameters are given in Table 1. The cross sectional view is given in Fig. 1. There are 18 CSR and 6 DSR,
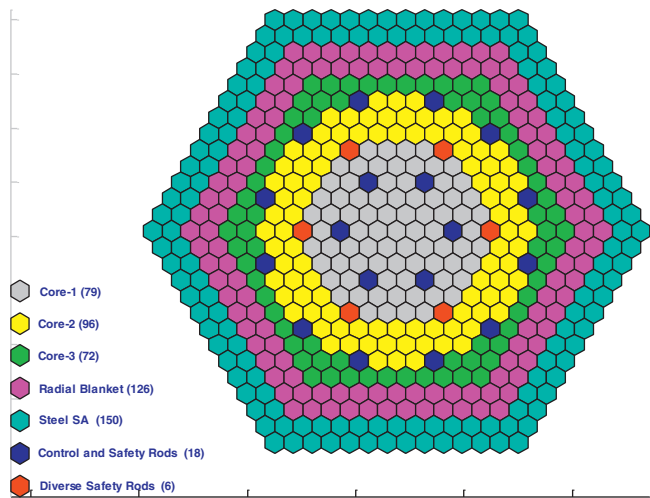
Fig. 1. Core configuration of 1000 MWe FBR.

making a total of 24 absorber rods. Natural B_4C absorber rods are expected to meet the reactivity requirements. Power distribution, reactivity worths associated with fuel Doppler and removal of fuel, clad and coolant are calculated based on two dimensional diffusion theory calculations using ABBN cross-section set (Riyas and Mohanakrishnan, 2009). Fuel pin diameter is chosen to be 8 mm to get higher breeding ratio. Correspondingly fuel volume fraction is higher and Na volume fraction is lower. Computed breeding ratio is 1.49. Details of the estimation of static parameters like breeding ratio, power distribution and sodium void reactivity effect have been reported earlier (Riyas and Mohanakrishnan, 2008). The delayed neutron fraction is calculated using the code PERT-ABBN that is based on first order perturbation theory, which is a modified version of NEWPERT (John, 1984).

3. Calculation methodology

Static and dynamic analyses are carried out using the code PREDIS (Harish et al., 1999). PREDIS is a multi-channel, single pin model code, where each flow channel is represented by a representative single fuel pin with its associated coolant flow and surrounding structure. The code uses point kinetics model for calculation of reactor power. Net reactivity is a sum of input reactivity and feedback reactivity. Heat transfer is calculated by using lumped parameter model. Though Fourier heat conduction model gives better accuracy in heat transfer studies, due to high fuel thermal conductivity and better gap conductance, the peak to average fuel temperature ratio is small (about 1.1 in metal as compared to 1.5 in oxide fuel). So lumped model analysis is considered to be adequate to carry out the heat transfer analysis.

Considered feedback reactivities are the axial fuel expansion, radial expansion of the core, clad and coolant expansion, Doppler feedback due to broadening of resonances, spacer pad expansion and coolant voiding. Fuel axial expansion is assumed to be free without any fuel clad interaction. Both control rod drive line expansion feedback and main vessel expansion feedback are ignored here. In pool type FBR design with top support for the vessel, control rod drive line expansion introduces negative reactivity (due to

insertion of control rods) with outlet coolant temperature increase. Vessel expansion introduces a positive reactivity (due to lowering of the elevation of the core top) with pool temperature increase. In PFBR design which is considered for the 500 MWe core, where SS316 LN has been used for control rod drive and main vessel, these two effects estimated to be 0.15 mm/°C change in sodium temperature. In a transient, as the coolant outlet temperature change and the pool temperature change are different, these two effects will compensate only partly. Also the time constants of these two effects are different and of the order of minutes (Tanigawa and Yamaguchi, 1990).

4. Steady state analysis

Based on the flow zoning (Puthiyavinayagam, 2010) the 1000 MWe core is divided into 9 radial zones – 7 zones in fuel and 2 zones in radial blanket. In axial direction, the core is divided into 10 zones. The lower and upper axial blankets are divided into 2 zones each. Thermo-physical parameters and kinetics parameters are given in Tables 2 and 3 respectively. Perturbation worth such as fuel, clad and coolant removal worth of both 500 MWe and 1000 MWe are given in Table 4 for comparisons. Doppler coefficients calculated in the temperature range of 653–863 °C in 500 MWe case and between 473 and 1100 °C in 1000 MWe case are also given in Table 4.

Static reactivity ρ is the combination of many reactivity contributions arises from change in temperature (Ott, 1988), when the power changes from one asymptotic state to another asymptotic state. The various effects which contribute to the reactivity coefficient are the Doppler effect, fuel and clad axial expansion, coolant expansion, core radial expansion or flowering, control rod drive line expansion, vessel expansion and grid plate expansion. Here the Doppler and fuel axial expansion feedbacks are calculated as a function of change in average fuel temperatures and their corresponding Doppler and fuel removal worth. With axial thermal expansion, axial boundary movement of the core also contributes to the axial expansion feedback. Similarly clad axial expansion feedback is calculated based on the change in average clad temperatures and its removal worth. Coolant expansion reactivity is calculated based on the bulk coolant expansion/voiding and its removal worth. Core radial thermal expansion is determined based on the coolant temperature at the spacer pad location and its feedback is calculated from the fuel and clad removal worth (due to density change). Similarly boundary movement of core-1 to core-2, core-2 to core-3 and core-3 to the radial blanket also contributes to the core radial expansion feedback. Core radial expansion feedbacks are calculated

Table 2
Thermo physical parameters of metal fuels.

Parameter	U–Pu–6%Zr
Fuel density (g/cm^3)	15.80
Smeared density (g/cm^3)	11.85
Linear expansion coefficient (°C^{-1})	19.7×10^{-6}
Thermal conductivity (W/cm/°C)	0.25
Specific heat (J/g/°C)	0.200
Melting point (°C)	1067
Gap conductance (W/cm^2/°C)	27.02
Boiling point (°C)	3932
Latent heat of fusion (J/g)	38
Latent heat of vaporisation (J/g)	1641

Table 3
Kinetic parameters of 1000 MWe (U–Pu–6%Zr) core.

j	1	2	3	4	5	6	β
β_j (pcm)	8.461	82.679	76.502	155.11	74.651	23.056	420
λ_j (s^{-1})	0.01298	0.03139	0.13525	0.34771	1.39565	3.8421	

Table 4
Perturbation reactivity worths in 500 MWe and 1000 MWe cores.

Component	500 MWe-worth (in pcm)	1000 MWe-worth (in pcm)
Fuel worth – core only	−37,729	−30,736
Steel worth – core only	4965	6060
Coolant worth – core only	2228(5.5$)	2419(5.8$)
Doppler worth – core only	−650	−505
Fuel worth – whole reactor	−37,231	−30,983
Steel worth – whole reactor	4190	5559
Coolant worth – whole reactor	2050(5.1$)	2357(5.6$)
Doppler worth – whole reactor	−748	−538

based on the cantilever bending model (Young and Budynas, 2002). Grid plate and vessel expansion is determined based on the change in inlet coolant temperature and their feedbacks are calculated from the corresponding fuel and clad removal worth. Control rod drive line expansion feedback is calculated based on outlet coolant temperature.

$\delta\rho$ is the net change in reactivity when the power transformed from the nominal value P_0 to P_1. Net change in reactivity is a combination of different reactivity effects as explained below (please see the nomenclature to get the meaning of individual term).

$$\delta\rho = \delta\rho_D + \delta\rho_{fax} + \delta\rho_{cax\text{-}expn} + \delta\rho_{Na} + \delta\rho_{rad} + \delta\rho_{rd} + \delta\rho_g + \delta\rho_v \quad (1)$$

Net axial reactivity feedback $\delta\rho_{fax} = \delta\rho_{fax\text{-}expn} + \delta\rho_{fax\text{-}bound}$

Radial expansion feedback is calculated by assuming flowering of the core due to heating up of the spacer pad buttons. It is calculated based on the increment in coolant temperature at the spacer pad location.

Core radial expansion feedback

$$\delta\rho_{rad} = \delta\rho_{frad\text{-}expn} + \delta\rho_{crad\text{-}expn} + \delta\rho_{core1\text{-}core2}$$
$$+ \delta\rho_{core2\text{-}core3} + \delta\rho_{core3\text{-}blkt}$$

Net change in reactivity from Eq. (1) is,

$$\delta\rho = \delta\rho_D + \delta\rho_{fax\text{-}expn} + \delta\rho_{cax\text{-}expn} + \delta\rho_{Na} + \delta\rho_{frad\text{-}expn} + \delta\rho_{crad\text{-}expn}$$
$$+ \delta\rho_{fax\text{-}bound} + \delta\rho_{core1\text{-}core2} + \delta\rho_{core2\text{-}core3} + \delta\rho_{core3\text{-}blkt} + \delta\rho_{rd}$$
$$+ \delta\rho_g + \delta\rho_v \quad (2)$$

Reactor core is divided into 'irn' number of radial channels and 'jx' number of axial nodes, and the reactor power is distributed in all radial and axial nodes as function of position. Temperature gradients are calculated between the initial and the final asymptotic state at all axial and radial locations. Power coefficient is calculated from the available material removal worth and temperature gradient. Net change in reactivity $\delta\rho$ is the combination of all $\delta\rho^{j,i}$ values at all $irn \times jx$ locations.

i.e., $\delta\rho = \sum_{i=1}^{irn}\sum_{j=1}^{jx} \delta\rho^{j,i}$

Reactivity feedback due to thermal expansion is,

$$\delta\rho^{j,i} = \Delta k^{j,i}\alpha\delta T^{j,i}$$

where $\Delta k^{j,i}$ is the removal worth of the chosen material, α is the thermal expansion coefficient, $\delta T^{j,i}$ is the change in temperature between two asymptotes. The boundary movement reactivity feedback,

$$\delta\rho_{fax\text{-}bound} = \Delta z\alpha_f\delta T_f^{j,i}C^i$$

$$\delta\rho_{core1\text{-}core2} = \sum_{i=1}^{irc1}\sum_{j=1}^{jx}\{[R_1 + (R^{i+1} - R^i)\alpha_s\delta T_{Na}^{jsp,i}W^j]^2 - R_1^2\}\frac{E_{1,2}^j}{2R_1 + 1}$$

$$\delta\rho_{core2\text{-}core3} = \sum_{i=irc1+1}^{irc2}\sum_{j=1}^{jx}\{[R_2 + (R^{i+1} - R^i)\alpha_s\delta T_{Na}^{jsp,i}W^j]^2 - R_2^2\}$$
$$\times \frac{E_{2,3}^j}{2R_2 + 1}$$

$$\delta\rho_{core3\text{-}blkt} = \sum_{i=1}^{irn}\sum_{j=1}^{jx}\{[R_c + (R^{i+1} - R^i)\alpha_s\delta T_{Na}^{jsp,i}W^j]^2 - R_c^2\}\frac{D^j}{2R_c + 1}$$

From Eq. (2) $\delta\rho^{j,i}$ for a particular j,i location is,

$$\delta\rho^{j,i} = \frac{\delta\rho_D}{\delta T}\delta T_f^{j,i} + \Delta k_f^{j,i}\alpha_f\delta T_f^{j,i} + \Delta k_s^{j,i}\alpha_s\delta T_s^{j,i} + 3\Delta k_c^{j,i}\alpha_{Na}\delta T_{Na}^{j,i}$$
$$+ 2\alpha_s\delta T_{Na}^{jsp,i}\Delta k_f^{j,i}W^j + 2\alpha_s\delta T_{Na}^{jsp,i}\Delta k_s^{j,i}W_j + \Delta z\alpha_f\delta T_f^{j,i}C^i$$
$$+ \{[R_1 + (R^{i+1} - R^i)\alpha_s\delta T_{Na}^{jsp,i}W^j]^2 - R_1^2\}\frac{E_{1,2}^j}{2R_1 + 1}$$
$$+ \{[R_2 + (R^{i+1} - R^i)\alpha_s\delta T_{Na}^{jsp,i}W^j]^2 - R_2^2\}\frac{E_{2,3}^j}{2R_2 + 1}$$
$$+ \{[R_c + (R^{i+1} - R^i)\alpha_s\delta T_{Na}^{jsp,i}W^j]^2 - R_c^2\}\frac{D^j}{2R_c + 1}$$
$$+ \alpha_{rd}\delta T_{Na} + \alpha_g\delta T_{Na\text{-}inlet} + \alpha_v\delta T_{Na\text{-}inlet} \quad (3)$$

Time constant of control rod drive line expansion, grid plate expansion and vessel expansions are considerably high. So their corresponding feedbacks are ignored in the present simulation. In the above equation higher order terms of $(R^{i+1} - R^i)\alpha_s T_c^{jsp,i}W^j$ is neglected, as it is expected to be very small. Eq. (3) is simplified in to,

$$\delta\rho^{j,i} = \left[\frac{\delta\rho_D}{\delta T} + \Delta k_f^{j,i}\alpha_f + \Delta z\alpha_f C^i\right]\delta T_f^{j,i} + \Delta k_s^{j,i}\alpha_s\delta T_s^{j,i}$$
$$+ 3\Delta k_c^{j,i}\alpha_{Na}\delta T_{Na}^{j,i} + \left[2\alpha_s\Delta k_f^{j,i}W^j + 2\alpha_s\Delta k_s^{j,i}W^j\right.$$
$$+ 2R_1(R^{i+1} - R^i)\alpha_s W^j\frac{E_{1,2}^j}{2R_1 + 1} + 2R_2(R^{i+1} - R^i)\alpha_s W^j$$
$$\left.\times \frac{E_{2,3}^j}{2R_2 + 1} + 2R_c(R^{i+1} - R^i)\alpha_s W^j\frac{D^j}{2R_c + 1}\right]\delta T_{Na}^{jsp,i} \quad (4)$$

From the above equation, change in reactivity is basically a function of change in fuel clad and coolant temperatures at different axial and radial locations between the two asymptotic states.

Based on lumped heat transfer model, temperature gradient between the initial state and the final asymptotic states when the power transformed from the nominal power P_0 to a final asymptotic power P_1 is,

$$\delta T_{Na}^{j,i} = \delta T_i + \sum_{k=1}^{j}\frac{\Delta z}{C_c\rho A_f v(i)}\delta q^{k,i} \quad (5)$$

$$\delta T_s^{j,i} = \delta T_i + \sum_{k=1}^{j}\frac{\Delta z}{C_c\rho A_f v(i)}\delta q^{k,i} + \frac{\delta q^{j,i}}{h_{sc}} \quad (6)$$

$$\delta T_f^{j,i} = \delta T_i + \sum_{k=1}^{j} \frac{\Delta z}{C_c \rho A_f v(i)} \delta q^{k,i} + \frac{\delta q^{j,i}}{h_{sc}} + \frac{\delta q^{j,i}}{h_{fs}} \tag{7}$$

δq in Eqs. (5)–(7) is the change in linear power between any two asymptotic states at a given spatial location, which is written as $q(P-1)$. Similarly, linear power to flow ratio $\delta q/v(i)$ is written as $(q/v(i))((P/F)-1)$. From Eqs. (5)–(7), Eq. (4) becomes,

$$\delta \rho^{j,i} = \left\{ \left[\frac{\delta \rho_D}{\delta T} + \Delta k_f^{j,i} \alpha_f + \Delta z \alpha_f C^i \right] \left(\frac{1}{h_{sc}} + \frac{1}{h_{fs}} \right) + \Delta k_s^{j,i} \alpha_s \frac{1}{h_{sc}} \right\}$$

$$\times q^{j,i}(P-1) + \left[\frac{\delta \rho_D}{\delta T} + \Delta k_f^{j,i} \alpha_f + \Delta z \alpha_f C^i + \Delta k_s^{j,i} \alpha_s \right.$$

$$+ 3\Delta k_c^{j,i} \alpha_{Na} \right] \sum_{k=1}^{j} \frac{\Delta z}{C_c \rho A_f} \frac{q^{k,i}}{v(i)} \left(\frac{P}{F} - 1 \right)$$

$$+ \left[2\alpha_s \Delta k_f^{j,i} W^j + 2\alpha_s \Delta k_s^{j,i} W^j + 2R_1(R^{i+1} - R^i)\alpha_s W^j \right.$$

$$\times \frac{E_{1,2}^j}{2R_1 + 1} + 2R_2(R^{i+1} - R^i)\alpha_s W^j \frac{E_{2,3}^j}{2R_2 + 1}$$

$$+ 2R_c(R^{i+1} - R^i)\alpha_s W^j \frac{D_j}{2R_c + 1} \right] \sum_{k=1}^{jsp} \frac{\Delta z}{C_c \rho A_f} \frac{q^{k,i}}{v(i)} \left(\frac{P}{F} - 1 \right)$$

$$+ \left[\frac{\delta \rho_D}{\delta T} + \Delta k_f^{j,i} \alpha_f + \Delta z \alpha_f C^i + \Delta k_s^{j,i} \alpha_s + 3\Delta k_c^{j,i} \alpha_{Na} \right.$$

$$+ 2\alpha_s \Delta k_f^{j,i} W^j + 2\alpha_s \Delta k_s^{j,i} W^j + 2R_1(R^{i+1} - R^i)\alpha_s W^j \frac{E_{1,2}^j}{2R_1 + 1}$$

$$+ 2R_2(R^{i+1} - R^i)\alpha_s W^j \frac{E_{2,3}^j}{2R_2 + 1}$$

$$+ 2R_c(R^{i+1} - R^i)\alpha_s W^j \frac{D_j}{2R_c + 1} \right] \delta T_i \tag{8}$$

Variables in Eq. (8) are the linear power and the coolant flow velocity. If thermo physical properties are assumed to be constant, change in reactivity at a given reactor location is purely a function of linear power and the flow velocity.

Quasi static reactivity balance (Wade and Chang, 1988) equation can be written as follows when the power goes from one steady state to another steady state.

$$\Delta \rho = (P-1)A + \left(\frac{P}{F} - 1 \right) B + \delta T_i C + \Delta \rho_{ext} \tag{9}$$

By comparing Eqs. (8) and (9), the coefficient A, B, C can be written as follows,

$$A = \left\{ \left[\frac{\delta \rho_D}{\delta T} + \Delta k_f^{j,i} \alpha_f + \Delta z \alpha_f C^i \right] \left(\frac{1}{h_{sc}} + \frac{1}{h_{fs}} \right) + \Delta k_s^{j,i} \alpha_s \frac{1}{h_{sc}} \right\} q^{j,i} \tag{10}$$

From Eq. (10), contribution of power-flow coefficient A comes from Doppler component, fuel axial expansion and boundary movement components. For a given change in linear power δq between two asymptotes, the coefficient A is a function of the Doppler worth, axial boundary movement worth and the thermo physical properties such as the linear expansion coefficient and the effective heat transfer h_{fs}. Considerable difference in Doppler coefficient between the oxide and metal fuel core arises due to change in neutron spectrum and fuel enrichment. The difference in effective

heat transfer between oxide and metal fuel arises due to the difference in fuel thermal conductivities and the bond gap conductance. Thermal conductivity of metal fuel is about 5–10 times more than the oxide fuel. Similarly, sodium bond gap conductance is about 27 times more than helium bond gap. Fuel axial thermal expansion is assumed to be free of clad temperature, so long as the fuel clad gap is open. Once the gap is closed, then fuel axial expansion is controlled by the clad expansion. On the other hand, clad temperature and its axial expansion is a function of change in linear power and change in power to flow value. Power-flow coefficient A explains the amount of reactivity vested from the fuel side.

$$B = \left[\frac{\delta \rho_D}{\delta T} + \Delta k_f^{j,i} \alpha_f + \Delta z \alpha_f C^i + \Delta k_s^{j,i} \alpha_s + 3\Delta k_c^{j,i} \alpha_{Na} \right]$$

$$\times \sum_{k=1}^{j} \frac{\Delta z}{C_c \rho A_f} \frac{q^{k,i}}{v(i)} + \left[2\alpha_s \Delta k_f^{j,i} W^j + 2\alpha_s \Delta k_s^{j,i} W^j \right.$$

$$+ 2R_1(R^{i+1} - R^i)\alpha_s W^j \frac{E_{1,2}^j}{2R_1 + 1} + 2R_2(R^{i+1} - R^i)\alpha_s W^j \frac{E_{2,3}^j}{2R_2 + 1}$$

$$+ 2R_c(R^{i+1} - R^i)\alpha_s W^j \frac{D_j}{2R_c + 1} \right] \sum_{k=1}^{jsp} \frac{\Delta z}{C_c \rho A_f} \frac{q^{k,i}}{v(i)} \tag{11}$$

From Eq. (11), for a given linear power "q" and the flow velocity $v(i)$ the power/flow coefficient B is contributed by the Doppler, both axial and radial boundary movement worth and the thermo physical properties such as the linear expansion coefficient and the rise in coolant temperature at all location. Rise in coolant temperature at the spacer location contributes to the flowering reactivity feedback. Power/flow coefficient B is the amount of reactivity vested from the coolant side.

$$C = \left[\frac{\delta \rho_D}{\delta T} + \Delta k_f^{j,i} \alpha_f + \Delta z \alpha_f C^i + \Delta k_s^{j,i} \alpha_s + 3\Delta k_c^{j,i} \alpha_{Na} + 2\alpha_s \Delta k_f^{j,i} W^j \right.$$

$$+ 2\alpha_s \Delta k_s^{j,i} W^j + 2R_1(R^{i+1} - R^i)\alpha_s W^j \frac{E_{1,2}^j}{2R_1 + 1} + 2R_2(R^{i+1} - R^i)$$

$$\times \alpha_s W^j \frac{E_{2,3}^j}{2R_2 + 1} + 2R_c(R^{i+1} - R^i)\alpha_s W^j \frac{D_j}{2R_c + 1} \right] \delta T_i \tag{12}$$

From Eq. (12), the inlet temperature coefficient C is contributed by the Doppler component, fuel & clad axial and radial expansions and fuel axial and radial boundary movement components. Reactivity feedback such as grid plate expansion arises from the change in inlet coolant temperature. Disturbance in the balance of plant (BOP) is the main cause of change in inlet coolant temperature. Inlet temperature coefficient C also contributes to the reactivity vested from the coolant side. In the present calculation inlet coolant temperatures are assumed to be a constant. So, the reactivity feedback contribution from grid plate expansion is ignored.

4.1. Power reactivity decrement from reactivity parameter

The reactivity parameters A, B and C are determined for each spatial node individually from Eqs. (10)–(12). Based on the reactor material worth, reactor is divided in to ten radial channel and fourteen nodes in the axial direction as it is done in the earlier calculations. Summation of all spatial node value gives the integral reactivity parameters A, B and C. The integral value of A, B and C gives a clear picture of the reactivity which is vested from the fuel side and the reactivity which is vested from the coolant side. But, in Eq. (9), change in reactivity has a linear relationship with power and power to flow ratio and inlet temperature. So, the solution may

Table 5
Comparisons of inherent safety parameter and power reactivity decrement.

| Parameters	Oxide core PFBR (500 MWe)	Metal core	
		500 MWe	1000 MWe
A (pcm)	−669.0	−112.0	−126.9
B (pcm)	−151.4	−124.1	−132.92
Power reactivity decrement ($A+B$) (pcm)	−820.4	−236.1	−259.8

not hold for large arbitrary change in reactivity. However, Eq. (9) encompass the scenario of all possible unprotected events in which reactor may get affected.

From Eqs. (10) and (11), A, B value of 500 MWe medium sized oxide and metal fuelled reactors are compared in Table 5. Both the reactors have almost same linear power and similar thermal hydraulic parameters such as the fuel pin size and flow area. Corresponding values of 1000 MWe is also presented in the same table.

The value $A+B$ is the power reactivity decrement. This is the amount of reactivity which has to be compensated with the addition of external positive reactivity when the reactor is taken from zero power to nominal power, or this much of reactivity comes back as a positive reactivity when the reactor goes to zero power from nominal power. From Table 5 it is seen that the power reactivity decrement is more in case of oxide fuel (PFBR) as compared to metal fuelled reactors of similar size. So, metal fuel can goes to sub-critical with comparatively smaller negative feedback reactivity. To protect the reactor against UTOP (Unprotected Transient Over Power) and to have a stable operations, it is advisable to have high Doppler or negative reactivity feedback. However in metal fuel reactors due to hard neutron spectrum, breeding is high. High breeding reduces burn-up reactivity swing which reduces the control rod requirement. Thus in metal fuel reactors positive reactivity addition during a UTOP and the severity of UTOPA is reduced. However, there are results available in the literature (Tsujimoto et al., 2001) to improve the Doppler coefficient and sodium void reactivity in metal fuel reactors without sacrificing much on the breeding ratio and burnup reactivity loss by adding moderating materials such as zirconium hydride.

In case of loss of flow, flow velocity runs down with the flow halving time (τ). When the flow comes down, core gets heated up and it introduces negative reactivity, reduces power. With power fuel temperature also decreases, which may reduce the magnitude of negative Doppler or Doppler contribution may change in to positive. This is purely depends upon the considered reactor system. On the other hand in metal fuelled reactors, the stored Doppler value is very small and also due to high thermal conductivity, the stored energy in the fuel is also very small (Chang, 2007). So, the Doppler contribution is almost closer to zero or negative. In oxide fuelled reactors stored Doppler coefficient is high and the difference in temperature between fuel and coolant is very high (about 900 °C). This difference makes the possibility of heat transfer from the fuel to coolant, thus there is a reduction in fuel temperature which turns the fuel axial expansion feedback and Doppler feedback in to positive. In metal fuel the difference in temperature between fuel and coolant is not so high (about 100 °C). This implies a mild rise in fuel temperature with a rise in coolant temperature during flow coast down. This is the reason why in metal fuel reactors both the Doppler feedback and the fuel axial expansion feedbacks are likely to be negative and it is positive in oxide fuel reactors.

When a reactor is designed with proper inherent safety parameters, for a given flow perturbation (flow reduction), positive reactivity of power reduction is balanced by the negative reactivity of core heat up and the reactivity asymptotically go to zero. When
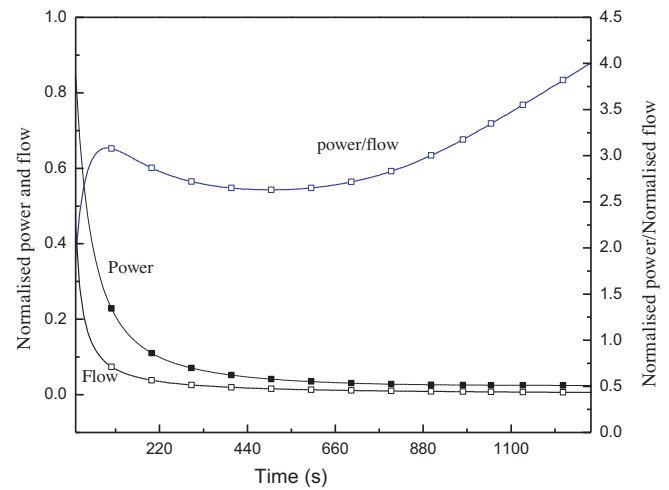
Fig. 2. Power, flow and the ratio of power to flow for ULOF analysis of 1000 MWe, with conservative decay heat estimation.

the flow decreases ultimately it may go to the natural circulation flow if the buoyancy force and the pressure drops across different locations are balanced properly. When the flow reduces to natural circulation, P/F value increases and the reactivity get balances; ultimately the power goes to zero. From Eq. (9) it is possible to determine the change in P/F value and also the change in outlet coolant temperature,

$$\frac{P}{F} = 1 + \frac{A}{B} \text{ and } \delta T_{out} = \Delta T_c \frac{\delta P}{F} = \frac{A}{B}\Delta T_c \quad (13)$$

Eq. (13) gives the idea of change in outlet coolant temperature, for a given change in P/F ratio. In case of ULOFA change in outlet coolant temperature will be minimal when B is greater than A. This is the case in metal core as shown in Table 5. That is when the amount of reactivity vested form coolant is more than the amount of reactivity vested from the fuel. Flow halving time is typically shorter than the time constant of delayed neutron precursors. With flow coast down when the power decreases, delayed neutron hold back may give a contribution. Delayed neutron hold back may also play a role in reactivity balance which is not considered in the present study. Based on Eq. (13) change in outlet coolant temperature is 159.4 °C. With this change, net outlet temperature is converged to 733 °C. There is about 150 °C margins to coolant saturation.

5. Transient analyses

Scenario of pump flow coast down (possibly initiated by power failure) with all the shut down rods unavailable is considered for the transient analyses. Reactivity feedbacks are the only parameters which controls the power response of the reactor. The coolant flow is assumed to be coasting with a flow halving time of 8 s. The flow (V) decrement is of the form

$$V(t) = \frac{V(0)}{1 + t/t},$$

where τ is the flow halving time. In case of 1000 MWe, after the initiation of flow reduction, the reactor becomes sub-critical and the power decreases continuously. Since the reactor is sub-critical throughout the transient, heat is principally generated from the decay of fission products after about 600 s. From Fig. 2, it can be seen that although both power and flow decrease continuously, the rate of fall of power is relatively smaller than that of flow. This leads to a rise in the ratio of power to flow during the first 80 s of the transient where the ratio is found to reach a value of 3.1. Thereafter
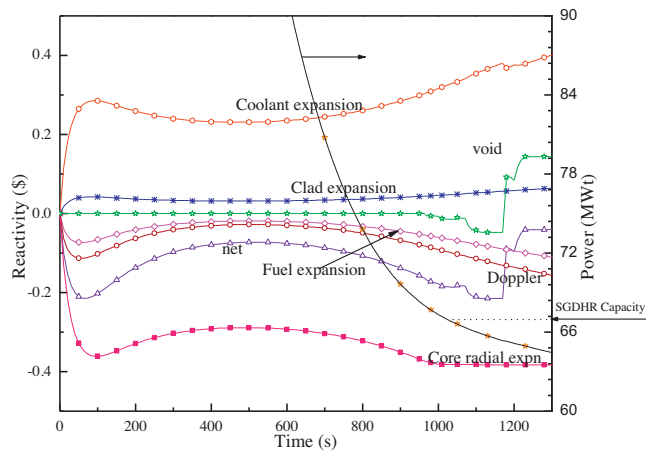
Fig. 3. Feedback reactivity of 1000 MWe ULOF analysis with conservative decay heat estimation.

the ratio decreases and there is a decrement in coolant, clad and fuel temperatures. The decrement in fuel temperature reduces the fuel expansion and Doppler resonance negative reactivity feedback which reduces the magnitude of net reactivity (Figs. 3 and 4). By that time (>600 s) fission power and flow are reduced further so that the total power is only the decay power. As the decay power decrease rate is smaller as compared to the flow decrease rate, power to flow ratio increases after about 600 s. It is important to consider the working of natural convection based SGDHRS. A formula has been fitted to estimate decay heat with time for the end of equilibrium cycle of PFBR which includes the contribution of fission products, actinides and also steel and sodium activation. The formula is

$$P_{cd} = 0.0631\, P_0 t^{-0.1322}$$

where t is time after shut down and P_0 is steady state nominal power. An uncertainty of 20% is also added which makes the decay heat estimate conservative. It is assumed that decay heat of metal fuelled FBR is same as oxide fuelled FBR. Reduction in flow with time increases fuel, clad and coolant temperature, and sodium boiling is initiated at 963 s in upper axial blanket of the third radial zone. Variation of reactivity and temperature with time is shown in Figs. 3 and 4 respectively. After the boiling initiation, two-phase flow hydrodynamics equations are solved to determine the void
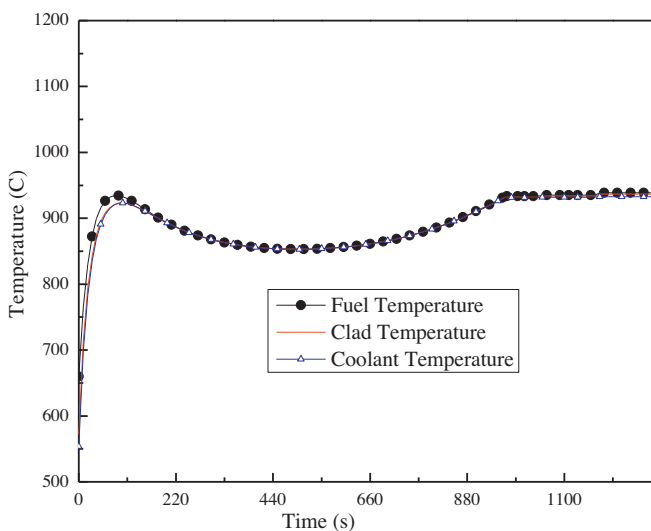
Fig. 4. Temperatures of 1000 MWe ULOF analysis with conservative decay heat estimation.
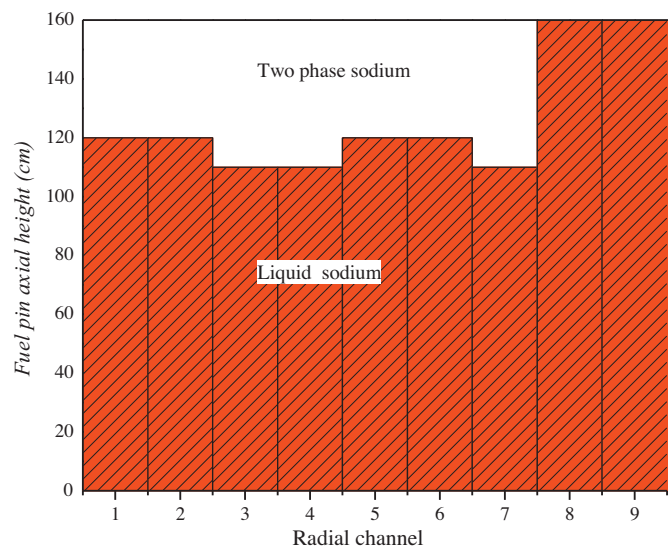
Fig. 5. Void distribution at 1200 s for 1000 MWe ULOF analysis with conservative decay heat estimation.

fraction at a given axial location. After that any heat input to the coolant will raise the void fraction. Initially, the void propagation in the downward axial direction is through initiation of boiling in the adjacent axial node. With time, initiation of sodium boiling is occurring in many other radial channels also. Since the boiling is initiated in the upper part of the core, where the corresponding reactivity worth is negative, the reactivity feedback is negative till substantial amount of void propagate downwards, where the void reactivity effect is positive. The regions in core and blanket where sodium is present as liquid and where both liquid and vapour phases are present at 1200 s are given in Fig. 5.

After 1180 s, contribution of void reactivity changes in to positive as the void propagates further down. The net reactivity is still negative due to the contribution of core radial expansion feedback. By 1180 s, the net power has dropped to 65 MWt, which is less than the SGDHRS capacity. The over all feedback and net reactivity is maintained negative throughout the ULOF analysis, till the SGDHRS takes over the heat transfer through natural convection even with conservative estimation of decay heat.
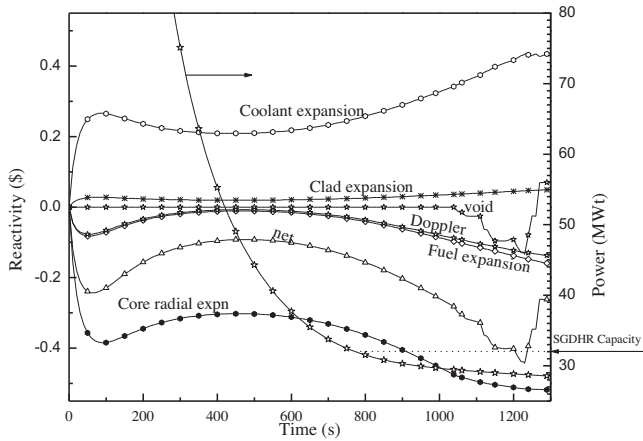
6. Sensitivity analysis

ULOF analyses of 1000 MWe metal fuel FBR is found to go to safe shutdown without any coolant boiling. Sensitivity analyses are carried out to ensure safe shutdown with considered uncertainties on reactivity feedback parameters. The sensitive parameters which affect the ULOF characteristic behaviour are seem to be overall radial expansion reactivity feedback and sodium expansion reactivity effect which compete with each other as shown in Fig. 3. So, it is required to carry out transient analysis by considering all relevant uncertainty factors as recommend by Mueller (1986) on reactivity feedback uncertainties. The sensitivity analyses are carried out using two different possibilities (Fig. 6).

6.1. Sensitivity analysis of 1000 MWe FBR

6.1.1. Enhanced sodium void reactivity and reduced core radial expansion reactivity feedback

To derive confidence on the inherent safety of 1000 MWe metal fuel FBR and to consider the calculation uncertainties, the core radial expansion coefficient is reduced to 80% and the sodium void reactivity effect is increased to 120%. ULOF initiates voiding at about
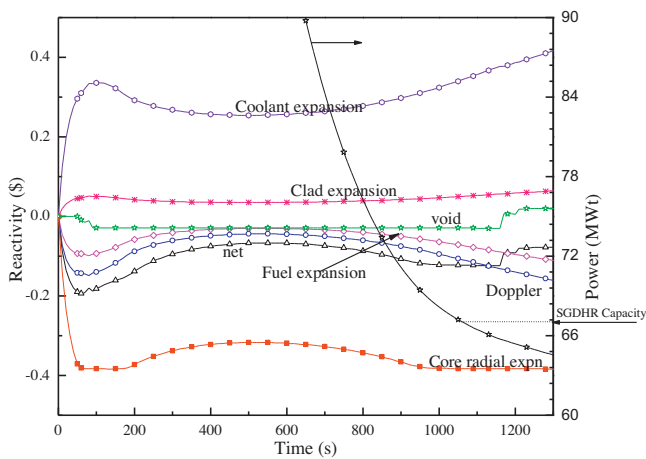
Fig. 6. Sensitivity analysis of 500 MWe with conservative decay heat estimation (80% core radial expansion reactivity feedback + 120% coolant void reactivity feedback).

38 s in upper axial blanket. With the initiation of voiding, the reactor is maintained in sub-critical state up to 71 s. After that, the void propagates in the downward direction towards the core centre and introduces positive void reactivity. When reactor power and fuel temperature increase with void propagation and its positive void feedback, initiation of fuel melt also occurs and more than 80% of melting is observed in about six to seven axial nodes of almost all the core radial channels. Similar scenario is found with considering 50% uncertainties in core radial expansion feedback.

6.1.2. Reduced core radial expansion reactivity feedback with nominal sodium void reactivity feedback

ULOF analyses are carried out with reduced core radial expansion reactivity feedback of about 80% and with nominal sodium expansion reactivity feedback (this corresponds to sensitivity study of a modified core with 20% reduced sodium void reactivity effect with 20% uncertainty added). Initiation of boiling occurs at about 50 s. Voiding occurs in top axial blanket, where the sodium void reactivity effect is negative. The net reactivity is also negative. Coolant void starts spreading in radial direction, where the sodium removal worth is negative. Coolant voiding does not propagate downward in axial direction. The net reactivity is negative and the reactor is maintained substantially sub critical even beyond the power crosses the SGDHRS capacity (∼1050 s) as shown in Fig. 7.

Fig. 7. Feedback reactivity of 1000 MWe ULOF analysis with conservative decay heat estimation (80% core radial expansion reactivity feedback + 100% coolant void reactivity feedback).
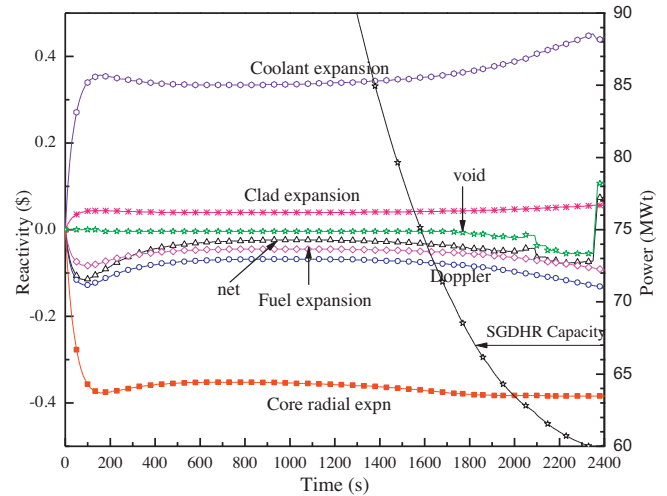
Fig. 8. Sensitivity analysis for flow halving time of 15 s (80% core radial expansion + 120% coolant void reactivity feedback).

So, if the sodium worth is reduced by 20% by design, even with reduced radial expansion reactivity feedback and enhanced sodium void reactivity – for accounting the uncertainties, the reactor goes to a safe shutdown state.

In summary, for 1000 MWe with the consideration of uncertainties, inherent safety parameters are not good enough in achieving passive shut down capability. Enhanced void reactivity effect (120%) and reduced core radial expansion (80%) resulted in fuel melting. There is a need for confirmation of the uncertainties in reactivity coefficients to ensure safety. But, if sodium worth is reduced by 20% by design, the reactor is expected to go to a safe shutdown state. For the present design, this means a reduction of sodium void reactivity effect from 5.8$ to 4.6$. By introducing a sodium plenum replacing upper axial blanket, it is possible to reduce the sodium void reactivity by more than 30%, which can make 1000 MWe reactor safe for ULOFA. But, that will reduce the breeding gain.

6.1.3. Enhanced sodium void reactivity and reduced core radial expansion reactivity feedback with extended flow halving time

Alternatively, it is considered to carry out the ULOF analyses by increasing the flow halving time without any design changes such as reducing the void coefficient with the reduced breeding gain. To ensure the safety of 1000 MWe reactor with extended flow coast down, ULOF analyses are carried out with 15 s flow halving time. Increment in flow halving delays the sodium boiling initiation, and its positive reactivity contribution. With 15 s, flow halving time, coolant boiling was initiated at 124 s. However, even with the initiation of voiding the reactor is maintained to be in sub-critical state. Reactivity components and power is shown in Fig. 8. At about 1850 s before the net reactivity change into positive, total power reduced to SGDHRS capacity. Similarly, considering 50% uncertainties on the core radial expansion also, the power reduced to SGDHRS capacity, before the net reactivity changes into positive. This study recommends the extended flow coast down (15 s instead of 8 s) to ensure the safe shutdown of 1000 MWe MFBR with considering uncertainties on reactivity feedback, without making any design changes such as reducing the sodium void coefficient and breeding gain.

7. Summery and conclusions

Static and dynamic studies of metal fuelled fast breeder reactors (MFBR) are carried out to verify the passive shutdown capability

and its inherent safety parameters. Static calculations are carried out to determine the vested reactivity feedback parameters from the fuel temperature rise and coolant temperature rise separately. Maximum coolant temperature of the reactor for a given initiating events are calculated based on the reactivity feedback parameters. It is found, reactivity decrement of metal fuel reactor is small as compared to oxide fuel of similar thermal output. From the static studies it is concluded that, metal fuel can go to sub-critical state with comparatively smaller negative feedback reactivity during Unprotected Loss of Flow Analysis (ULOFA), and its maximum coolant temperature is below its saturation point.

Transient analyses are carried out on a 1000 MWe metal cores to find out the passive shutdown capability of the reactor, and its inherent safety parameters. From the analysis, it is found that nominal behaviours of 1000 MWe core under ULOFA is benign. After ULOFA, the over all reactivity remains negative till the power reduces below SGDHRS capacity. From the analysis, it is found that the sensitive parameters which affect the ULOF characteristic behaviour are the overall radial expansion reactivity feedback and sodium void reactivity effect. Sensitivity analyses are carried out to ensure the safe shutdown with considered uncertainties on these reactivity feedback parameters.

Sensitivity studies with 8 s flow halving time shows there is relatively a fast initiation of sodium voiding and the core heads for disassembly in less than 100 s. However if the increased sodium void reactivity effect is not considered along with the reduced radial expansion reactivity feedback, then the reactor reaches Safety Grade Decay Heat Removal (SGDHRS) capacity power level at about 1000 s in a sub-critical state. These studies indicate that there is a need to restrict the sodium void reactivity effect of large metal fuelled FBR for its safety. In the present case, reduction of 5.8–4.6\$ is studied.

Alternatively, thought was given by increasing the flow halving time without any design changes such as reducing the void coefficient and breeding gain. ULOF analyses are carried out with 15 s flow halving time. Increment in flow halving delays the sodium boiling initiation. Reactor power reduced to SGDHRS capacity in a sub-critical state with considering all uncertainties on core radial expansion and sodium void coefficient.

Based on these studies it is concluded that, either reducing the sodium void reactivity effect or increasing the flow halving time take the 1000 MWe MFBR to safe shutdown to avoid cliff edge effects.

Acknowledgements

References

Cahalan, J., et al., 1990. Performance of metal and oxide fuels during accidents in a large liquid metal cooled reactor. In: International Fast Reactor Safety Meeting, Snowbird, USA.

Chang, Y., I.L., 2007. Technical rationale for metal fuel in fast reactors. J. Nucl. Eng. Technol. 39 (3), 161.

Chetal, S.C., et al., 2006. The design of the prototype fast breeder reactor. Nucl. Eng. Des. 236, 852–860.

Coffield, et al., 1986. How to achieve inherent safety capability in a large LMFBR. Trans. Am. Nucl. Soc. 53, 304.

Devan, K., 2003. An Interface between CONSYST/ABBN-93 and IGCAR Diffusion Theory Codes. RPD/NDS/90, IGCAR Report.

Harish, R., Sathiyasheela, T., Srinivasan, G.S., Om Pal Singh, 1999. KALDIS: A Computer Code System for Core Disruptive Accident Analysis of Fast Reactors, IGC – 208.

Harish, R., et al., 2009. A comparative study of unprotected loss of flow accidents in 500 MWe FBR metal cores with PFBR oxide core. Ann. Nucl. Energy 36, 1003.

Hummel, H.H., Okrent, D., 1970. Reactivity Coefficients in Large Fast Power Reactors. ANS Publication, Hinsdale.

IAEA-TECDOC-1623, 2010. BN-600 Hybrid Core Benchmark Analyses, Results of a CRP on Updated Codes and Methods to Reduce the Calculational Uncertainties of the LMFR Reactivity Effects, IAEA report.

John T.M., 1984. NEWPERT – Perturbation Code for Two Dimensional Diffusion Equations. REDG/01150/RP-253, REDG/01150/RP-253, IGCAR Report, Kalpakkam.

Lehto, W.K., et al., 1987. Safety analysis for the loss-of-flow and loss-of-heat sink without scram tests in EBR-II. Nucl. Eng. Des. 101, 35–44.

Manturov, G.N., 1997. ABBN-93 group data library Part I: nuclear data for the calculation of neutron and photon radiation functions INDC (CCP-409). IAEA, Vienna.

Mueller, C.J., 1986. Impacts of reactivity feedback uncertainties on inherent shutdown in innovative designs. Trans. Am. Nucl. Soc. 53, 305.

Singh, O.P., Ponpandi, S., Harish, R., Singh, R.S., 1993. Response to small reactivity perturbations in an oxide and metal fuelled medium sized LMFBR. Ann. Nucl. Energy 20 (5), 315–319.

Singh, O.P., Harish, R., Ponpandi, S., Rao, P.B., Singh, R.S., 1994. Analysis of passive shutdown capability of loss of flow accident in a medium sized LMFBR. Annals of Nuclear Energy 21 (3), 165–170.

Singh, O.P., Harish, R., 2002. Energetics of core disruptive accident for different fuels for a medium sized fast reactor. Annals of Nuclear Energy 29, 673.

Ott, K.O., 1988. Inherent shutdown capabilities of metal-fueled liquid metal cooled reactors during unscrammed loss of flow and loss of heat sink incidents. Nucl. Sci. Eng. 99 (1), 13–27.

Planchon, H.P. et al., 1987. Implications of the EBR-II inherent safety demonstration test. Nucl. Eng. Des. 101 (1), 75–90.

Puthiyavinayagam, P., 2010. Communication on flow zoning for 1000 MWe metal core, dated 16 February.

Riyas, A., Mohanakrishnan, P., 2008. Studies on physics parameters of metal (U–Pu–Zr) fuelled FBR cores. Ann. Nucl. Energy 35, 87–92.

Riyas, A., Mohanakrishnan, P., 2009. 1000 MWe Metallic Fuelled FBR with Two Rows of Radial Blanket, REG/RPD/CPS/83, IGCAR Report, Kalpakkam.

Royl, P., et al., 1990. Influence of metal and oxide fuel behavior on the ULOF accident in 3500 MWth heterogeneous LMR cores and comparison with other large cores. In: International Fast Reactor Safety Meeting, Snowbird, USA.

Sathiyasheela, Riyas, T., Mohanakrishnan, A., Chetal, P., Baldev Raj, S.C., 2011. Comparative study of unprotected loss of flow accident analysis of 1000 MWe and 500 MWe Fast Breeder Reactor Metal (FBR-M) cores and their inherent safety. Annals of Nuclear Energy 38, 1065–1073.

Sathiyasheela, T., Mohanakrishnan, P., 2011. Power co-efficient using lumped heat transfer model, REG/RPD/NDS/SAS-213.

Tanigawa, S., Yamaguchi, K., 1990. Investigation of passive safety performance of a mixed-oxide fueled 1000 MWe LMFBR under ATWS conditions. In: International Fast Reactor Safety Meeting, Snowbird, USA.

Tsujimoto, K., et al., 2001. Improvement of reactivity coefficients of metallic fuel LMFBR by adding moderating material. Annals of Nuclear Energy, 831–855.

Wade, D.C., Chang, Y.I., 1988. The integral fast reactor concept: physics of operation and safety. Nucl. Sci. Eng. 100, 507–524.

Wade, D.C., Fujita, E.K., 1989. Trends versus reactor size of passive reactivity shutdown and control performance. Nucl. Sci. Eng. 103, 182–195.

Wade, D.C., Wigeland, R.A., Hill, D.J., 1997. The safety of the IFR. Prog. Nucl. Energy 31 (1–2), 63–82.

Wigeland, R., Cahalan, J., 2009. Fast reactor fuel type and safety performance. In: Proceedings of Global 2009, Paris, France, September 6–11 (Paper 9445).

Yokoo, T., Ohta, H., 2002. ULOF and UTOP analyses of a large metal fuel FBR core using a detailed calculation system. J. Nucl. Sci. Technol. 38 (6), 444–452.

Young, W.C., Budynas, R.G., 2002. Roark's Formulas for Stress and Strain, 7th ed. McGraw-Hill, New York, p. 189.